FEIIC International Journal of Engineering and Technology

Research Article

Electrochemical Performance of Bimetallic Silver-Gold Nanoparticles Decorated on Reduced Graphene Oxide for Glucose Detection

Faizah Md Yasin[1,2,*], Nur Atikah Ali[1], and Shafreeza Sobri[2]

[1] Institute of Nanoscience and Nanotechnology, Universiti Putra Malaysia, 43400, UPM Serdang, Selangor, Malaysia

[2] Department of Chemical and Environmental Engineering, Faculty of Engineering, Universiti Putra Malaysia, 43400, UPM Serdang, Selangor, Malaysia

*Corresponding author: fmy@upm.edu.my

ABSTRACT

In this study, one pot synthesis of bimetallic silver gold nanoparticles (AgAu NPs) decorated with reduced graphene oxide for glucose detection application is reported. An improved Hummers method was used to synthesize the graphene oxide (GO), which was later chemically reduced to obtain reduced graphene oxide (rGO). Meanwhile, a chemical reduction approach was adopted to prepare the AgAu/rGO nanohybrids: $HAuCl_4 \cdot 2H_2O$, $AgNO_3$, and rGO solutions were refluxed at 90°C with addition of trisodium citrate as a reducing agent. Morphological features and other physicochemical properties of the synthesized AgAu/rGO nanohybrids were evaluated using a battery of characterization technique. Raman spectra analysis confirmed the formation of GO and rGO. Appearance of new absorption peak of the UV-Vis spectra originating from the sp^2 hybridization in carbon network being restored indicated a successful reduction of GO to rGO. The absorption peaks appeared blue-shifted compared to rGO suggested a stronger interaction between bimetallic nanoparticles and rGO. High resolution transmission electron microscopy images revealed that GO and rGO both have wrinkles and crumble silk morphologies. After being decorated with AgAu/rGO, a well-dispersed of spherical AgAu nanoparticles with an average particle size of 40 nm were observed on the rGO surface, affecting the sensor performance toward glucose compared to rGO. For the sensor performance, the fabricated AgAu/rGO electrode exhibited glucose sensitivity of 428.1 $\mu A \cdot mM^{-1} \cdot cm^{-2}$ (~8 times higher than pristine rGO) and wide detecting linear range toward glucose up to 18 mM. Thus, AgAu/rGO may serve as a platform for future biosensors study for fast and responsive non-enzymatic glucose sensors.

Keywords. Bimetallic nanoparticles, reduced graphene oxide, sensors

1. INTRODUCTION

Graphene as one attractive carbon allotropes has gained a significant advancement among researchers after its discovery by Geim and Novoselov in 2004. Graphene is a flat monolayer of sp^2 - bonded carbon atoms tightly packed into a two-dimensional (2D) honeycomb lattice structure and considered as the thinnest material in the universe [1,2]. Due to its extraordinary properties such as large surface area, A (2,630 $m^2.g^{-1}$), high electrical conductivity and chemical stability, low cost and good flexibility [3], have made graphene as an ideal substrate for stabilizing, anchoring metal nanoparticles [4] and a rising element for various field of application such as nanoelectronics [5], energy materials [6], and biomedical [7]. Reduced graphene oxide (rGO) is a chemically or thermally treated derivative of graphene oxide (GO), obtained through the partial removal of oxygen-containing functional groups such as hydroxyl, epoxy, carbonyl and carboxyl moieties from the GO surface. Graphene oxide itself is typically synthesized from graphite via oxidative methods such as the Hummers' method, which introduces abundant oxygen functionalities and disrupts the extended sp^2 carbon network [8]. The subsequent reduction process aims to restore the conjugated π-electron system and electrical conductivity while retaining a certain amount of residual functional groups and structural defects. As reported by Stankovich et al. [9], chemical reduction of

exfoliated graphite oxide significantly enhances conductivity due to the re-establishment of the sp^2 carbon framework. Compared to pristine graphene, rGO possesses a high specific surface area, improved electrical conductivity, good mechanical flexibility, and abundant defect sites that serve as active centers for nanoparticle anchoring. These unique physicochemical properties make rGO an excellent supporting matrix for metal and bimetallic nanoparticles, facilitating enhanced electron transfer and synergistic electrocatalytic performance in sensing applications, including glucose detection [10,11].

In recent years, there have been numerous research focused on the development of rapid, sensitive and precise glucose sensors for glucose monitoring and is no longer relevant in the clinical sectors but also in the food industry, bioprocess and other [12]. In 2010, Toghill and Compton [13] stated that the enzyme and non-enzyme electrochemical sensors glucose sensing approach has been studied over the past decade have given a good insight into the biomedical field. As is known, enzyme-based glucose sensors have a good level of sensitivity. However, these enzyme-based sensors have sensor instability that are influenced by other factors such as environmental temperature and pH where it will cause false alarms and improper blood glucose readings. Hence, continuous research efforts on non-enzyme glucose sensors are actively being carried out and aims to enhance the weaknesses found in traditional enzymatic sensors. Most non-enzymatic sensors are advantageous in terms of structural simplicity, quality control for mass production, and they are free from oxygen limits where oxygen content can modulate sensor sensitivity and cause a non-linear response and less sensitive to glucose concentration.

Most non-enzymatic glucose sensors offer clear practical advantages over enzymatic systems, particularly in terms of stability and operational robustness. Conventional glucose biosensors commonly employ glucose oxidase (GOx) as the biological catalyst. Although GOx provides high selectivity, its catalytic activity is strongly influenced by environmental conditions such as temperature and pH. Even slight deviations from the optimal range can lead to partial denaturation or reduced enzyme activity, ultimately affecting sensitivity and reproducibility. In addition, first-generation enzymatic sensors rely on dissolved oxygen as a co-reactant, meaning that fluctuations in oxygen concentration may cause non-linear responses and compromise detection accuracy, especially under low-oxygen conditions. These inherent limitations of enzyme-based systems have been widely discussed in the literature, including the work of Wilson and Turner (1992) and later reviewed by Wang (2008) [14,15].

In contrast, non-enzymatic glucose sensors eliminate the use of biological components and instead rely on the direct electro-oxidation of glucose at the electrode surface. This fundamental difference allows the sensor to operate over a broader range of temperature and pH conditions without the risk of catalyst degradation. Noble metals such as Au and Ag are known to exhibit strong catalytic activity toward glucose oxidation, particularly in alkaline media, while maintaining excellent chemical and thermal stability. As highlighted by Toghill and Compton (2010), metal-based non-enzymatic systems generally demonstrate improved durability and longer operational lifetimes compared to enzymatic counterparts [13].

In the present system, the combination of Ag and Au in a bimetallic configuration is expected to further enhance catalytic performance through synergistic electronic effects. The interaction between the two metals can modify surface electronic properties, facilitate glucose adsorption and accelerate electron transfer during oxidation. When these nanoparticles are uniformly decorated on reduced graphene oxide (rGO), the overall performance is further improved. The high conductivity and large surface area of rGO provide an efficient electron transport pathway and abundant anchoring sites, minimizing nanoparticle aggregation while maximizing exposure of active sites. Such noble metal-carbon nanocomposites have been reported to significantly enhance electrocatalytic efficiency in glucose sensing applications [16]. Therefore, integrating Ag–Au bimetallic nanoparticles with rGO not only addresses the temperature, pH, and oxygen-dependence limitations associated with enzymatic glucose sensors but also offers enhanced catalytic activity, structural stability, and practical suitability for long-term sensing applications.

In the current work, a simple chemical reduction approach was employed to synthesize rGO and bimetallic Ag-Au nanoparticles decorated on rGO for non-enzymatic glucose detection. Ag and Au were selected over other noble metals such as Pt, Pd, and Rh due to their strong catalytic activity toward glucose oxidation in alkaline media, lower susceptibility to surface poisoning, and comparatively lower cost, making them more practical for sensor fabrication. Our findings showed that bimetallic Ag-Au nanoparticles decorated on rGO exhibited excellent sensitivity in detecting glucose concentrations up to 18 mM compared to rGO alone. These results indicate the strong potential of Ag-Au/rGO nanocomposites for the development of non-enzymatic glucose sensors, enabling more reliable glucose monitoring so that patients can receive appropriate treatment to maintain normal glucose levels and reduce the risk of severe complications.

2. MATERIALS AND METHODS

2.1. Chemicals

Graphite powder (99.99%), Gold (III) Chloride trihydrate ($HAuCl_4$), trisodium citrate ($Na_3C_6H_5O_7$), Silver Nitrate ($AgNO_3$) with 99.99% purity are procure from Sigma Aldrich. All the other chemicals used were of analytical grade and without further purification. Ultrapure water (18.2 MΩ·cm at 25°C) was obtained using a Millipore Milli-Q purification system to ensure the removal of ionic and organic contaminants prior to synthesis and electrochemical measurements.

2.2. Preparation of Reduced Graphene Oxide

An Improved Hummers method was used to synthesis graphene oxide (GO) using graphite powder as stated in [18]. 9:1 mixture of concentrated H_2SO_4/H_3PO_4 (360:40 mL) was added to a mixture contain of 3.0 grams of graphite powder and stirred well. While stirring, 18 grams of $KMnO_4$ was added gradually and slowly to the above reaction mixture, a slight heat was released with a temperature of around 35 - 40°C. Then, the reaction mixture was heated up to 50°C and the reaction continued stirring for 12 hours and cooled to room temperature for 1 hour and then poured onto ice cube (~ 400 mL) with addition of 30% H_2O_2 (3 mL) to ensure completion reaction with $KMnO_4$. In a few moments, the colour of the reaction mixture was changed to bright yellow. A centrifugation technique at 4,000 RPM was used for decantation of the supernatant for the above mixture. The suspension is washed in succession with 200 mL of water, HCl and acetone (2 times) to remove any impurities with centrifugation technique. Lastly, the suspension was coagulated with 200 mL of ether, and the resulting suspension was filtered over filter paper. The solid obtained on the filter was vacuum dried overnight at room temperature. To obtain reduced graphene oxide (rGO), 25 mg of GO was dispersed in 100 mL ultrapure water, and sonicated. Then, 0.5 g of sodium citrate was added to the solution and refluxed at 90°C for 12 hr with water condenser in an oil bath while stirring. The solution was then cooled down to room temperature to get reduced graphene oxide solution.

2.3. Preparation of AgAu/rGO

To obtained AgAu/rGO, 2 mL of 1% (w/v) of sodium citrate aqueous solution was added to a mixture of 20 mL of reduced graphene oxide stock solution and equal volume of $HAuCl_4$ (5 mL) and $AgNO_3$ (5 mL) aqueous solution refluxed at 90°C. The solution was constantly stirred for 20 minutes until reddish black colour dispersion appeared. All the solutions were centrifuged 3 times at 10,000 RPM with ultrapure water to remove undesired products.

2.4. Fabrication of Indium Tin Oxide (ITO) Glass Electrode with Nanohybrids

Indium tin oxide glass in original size of 2 cm × 2 cm was purchased from Xinyan Technology Company, China. Each piece of indium tin oxide glass was cut into 1 cm × 2 cm size using diamond cutter. Before the modification, indium tin oxide glass was ultra-sonicated subsequently in acetone solution for 20 min, ethanol solution 5 min, and ultrapure water for 5 minutes to remove any organic pollutant and contaminants. After that, the indium tin oxide glass was dried with blowing nitrogen stream [19]. Next, 0.5 mL ultrapure water was added into the synthesized rGO and AgAu/rGO nanohybrids and then sonicated each of them for 30 minutes to obtain homogenous dispersion. Following this, 50 µL of dispersion was dropped cast onto the clean indium tin oxide glass electrode and dried at room temperature.

2.5. Characterization

High-resolution transmission electron microscope measurements were done on a JEOL JEM 2100F Field Emission Transmission Electron Microscope (Japan) with an accelerating voltage of 200 kV to obtained nano-scales images of rGO and the nanohybrids. Samples for HRTEM characterization were prepared by dropping the prepared solution onto carbon coated copper grid and dried under table lamp. X-ray diffraction (XRD, Shimadzu XRD 6000, Japan) at 30 kV and 30 mA of Cu-Kα (radiation source λ = 1.5406 Å) was utilized to determine the crystalline structure of the prepared nanocomposites. UV-Vis detection was carried out on a Perkin Elmer lambda 35 to obtained absorption spectra of aqueous solutions (GO, rGO, and Ag/rGO, Au/rGO and AgAu/rGO) in the wavelength ranging from 200 nm to 700 nm. The Raman spectra of the rGO were obtained using WITec GmbH alpha 300R Raman spectrometer in the back scattering mode using Ar-ion laser (λ = 531.9 nm) as excitation source.

2.6. Electrochemical Measurements

Autolab PGSTAT-302N potentiostat / galvanostat has been used to investigate the electrochemical activity of the modified working electrodes toward glucose detection by using chronoamperometry. The electrochemical experiments were conducted in a three-electrode electrochemical cell system consisting of indium tin oxide (ITO) glass as a working electrode (A = 1 cm^2), platinum as the counter electrode and Ag/AgCl as the reference electrode at room temperature. 0.1 M phosphate buffer solution at pH 7.4 was used as a supporting electrolyte in the electrochemical experiments. Stock solutions of glucose ($C_6H_{12}O_6$) from 0 mM until 18 mM were freshly prepared by using ultrapure water and purged with nitrogen gas before starting each experiment [17].

After fabricating each modified electrodes, cyclic voltammetry (CV) was performed without and with glucose (0 mM and 4 mM) at scan rate of 50 $mV.s^{-1}$ between −0.1 V and +0.30 V and repeated for at least 3 times in 0.1 M PBS solutions. In addition, the electrolyte was purged with nitrogen gas at least 5 minutes prior to each electrochemical measurement. A chronoamperometry measurement was carried out in a 0.1 M PBS solution at an optimal potential of +0.20 V, +0.25 V and +0.30 V. The best potential will be chosen to evaluate each of the modified electrodes response toward glucose concentration from 0 mM to 18 mM.

3. RESULTS AND DISCUSSION

Figure 1 represents a Raman spectroscopy of the GO and rGO respectively. The Raman Spectrum of GO and rGO is characterized by two main modes of vibrations D and G band as shown. D band arising from a breathing mode of k-phonon of A1g symmetry corresponds to defects and staging disorder in C atoms, whereas the G band represent E2g phonons from in plane vibration of sp2 carbon atoms [20], [21]. The degree of ordered and disordered crystal structures of carbon can be calculated from the intensity ratio (ID/IG) between D and G bands [22], [23].

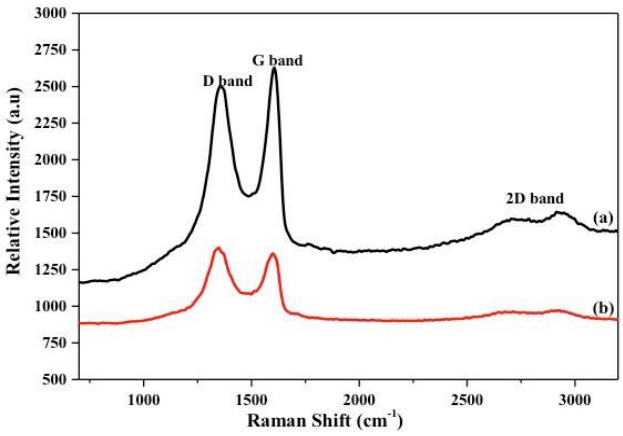

Figure 1. Raman spectra of (a) GO, (b) rGO

Table 1 shows the intensity ratio of the D and G band (ID/IG) of GO and rGO. For GO, (ID/IG) is 0.95. After reduction by sodium citrate, the ID/IG ratio of rGO increased to 1.03, respectively, hence confirming the formation of new graphitic domain during the reduction process of GO to rGO [24]. A broadened 2D peak was observed in ~2,750 cm^{-1} attributed to the presence of larger C=C bond. There is a blue shift in the 2D band peak position in the rGO around 2,713 cm^{-1} compared with GO around 2,705 cm^{-1}. These results are almost similar with the work of Gebreegziabher and co-workers, in which these 2D peaks show the presence of larger C=C domain in the rGO than GO and it tend to have a higher degree of crystallinity by observing the red shift in the D and G band position in rGO with respect to GO [25].

Table 1. Comparison of D band, G band, 2d band, ID/IG and I2D/IG value of GO and rGO

Material	D band (cm^{-1})	G band (cm^{-1})	2D band (cm^{-1})	I_D/I_G value	I_{2D}/I_G value
GO	1,355	1,600	2,758	0.95	0.60
rGO	1,350	1,605	2,769	1.03	0.71

Figure 2 reveals the UV-vis spectra of aqueous dispersion of the GO and rGO. In Figure 2 the spectrum for GO shows two characteristic peaks. The first peak was found at 230 nm attributed to the π - π* transitions of the aromatic C=C bonds, and a shoulder peak at 300 nm was observed and corresponding to n - π* transitions of the carbonyl C=O bonds which the result obtained from the analysis are along with the previous experiment [26]. Figure 2 shows an absorption peak at 230 nm was found to be red shifted to ~260 nm. These results indicate there is an increase in electronic conjugation, which is typical of the graphite and graphical structures that has been initiated [27][28]. The disappearance of shoulder peak at 300 nm suggesting that the sp^2 carbon network within reduced graphene oxide (rGO) is being restored after the reduction of GO [29][30][31].

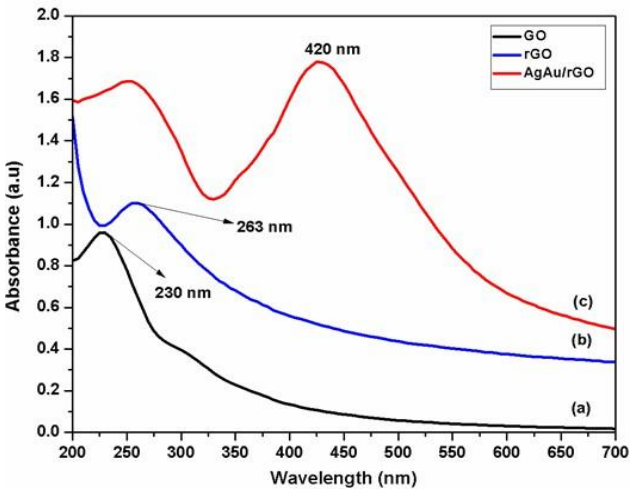

Figure 2. UV-Vis spectr of (a) GO, (b) rGO, and (c) AgAu/rGO

Figure 2 shows UV-Vis spectrum of AgAu/rGO. The absorption peak of reduced graphene oxide had been noticed to blueshift to ~ 256 nm due to the charge transfer interaction between the nanoparticles and reduced graphene oxide [32–34]. The typical wavelength for maximum absorption of the plasmon resonance for silver nanoparticles is approximately at 400 nm to 420 nm [35]. For gold nanoparticles, the standard wavelength for the maximum absorption peak is about 520 nm to 540 nm depending on the shapes and size of the nanoparticles [36]. The UV–Vis spectrum of AgAu/rGO shows a broad absorption peak at 430 nm respectively and is nearly to the Surface Plasmon Resonance (SPR) arithmetic mean value of Ag NPs at 425 nm [32], however a bit far from the standard absorption peak Au NPs at 520 nm. The absence of a distinct Au SPR peak at ~520-540 nm can be attributed to the formation of bimetallic Ag-Au nanoparticles rather than separate monometallic particles.

In alloyed Ag-Au systems, strong electronic coupling between Ag and Au leads to a single SPR band located between the characteristic positions of pure Ag and pure Au, depending on composition and electronic interaction, rather than two independent peaks, [37]. In addition, the SPR position is highly dependent on nanoparticle size, shape, and dielectric environment; therefore, variations in morphology and alloy structure in Ag-Au nanostructures can shift and broaden the plasmon band compared to their respective single-metal counterparts,[38]. Consequently, the observed broad peak at ~430 nm is consistent with the formation of Ag-Au bimetallic nanoparticles supported on rGO rather than isolated Au nanoparticles [39].

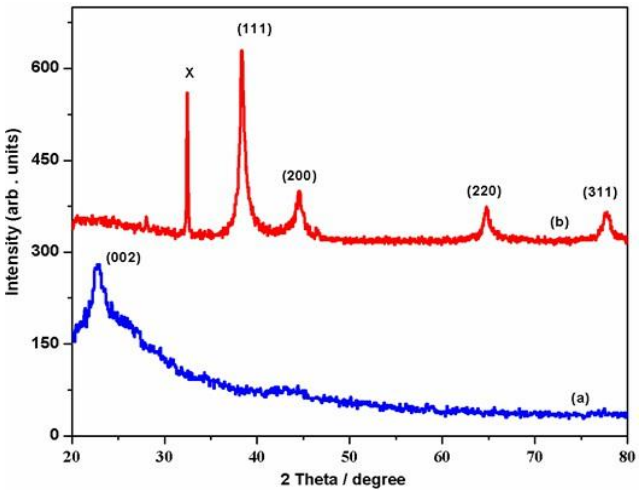

Figure 3. XRD analysis of (a) rGO, and (b) AgAu/rGO

For rGO, XRD pattern shows a broad diffraction peak at 2 theta, 2θ = 23°, as shown in Figure 3, attributed to (002) Bragg's reflection of the graphitic structure in which the finding is in good accordance with the research by Ju with co-researchers. According to their findings, the XRD results of rGO are closely related to the reduction process of GO and a process to eliminate intercalated of water molecules and the oxide group such as hydroxyl and carboxyl groups. However, upon further reduction, the broad peak at 2θ = 23° disappeared after the decoration with Ag, Au and AgAu bimetallic nanoparticles. Hence, the functionalization of the rGO surface with the Ag and Au nanoparticles might prevent the graphene sheets from restacking [40]. The prominent diffraction peaks were spotted for Ag, Au and AgAu bimetallic nanoparticles, which were situated at 2θ values of 38.1°, 44.5°, 64.5°, and 77.7°. The obtaining results is similar with the findings of Khalil and co-researchers [41]. All the four peaks corresponded to standard Bragg's reflections (111), (200), (220) and (311) which are identical with the crystalline planes of face centered cubic (fcc) lattice of Ag and Au nanoparticles. Hence, the broadening of Bragg's peaks suggested the formation of nanoparticles [42].

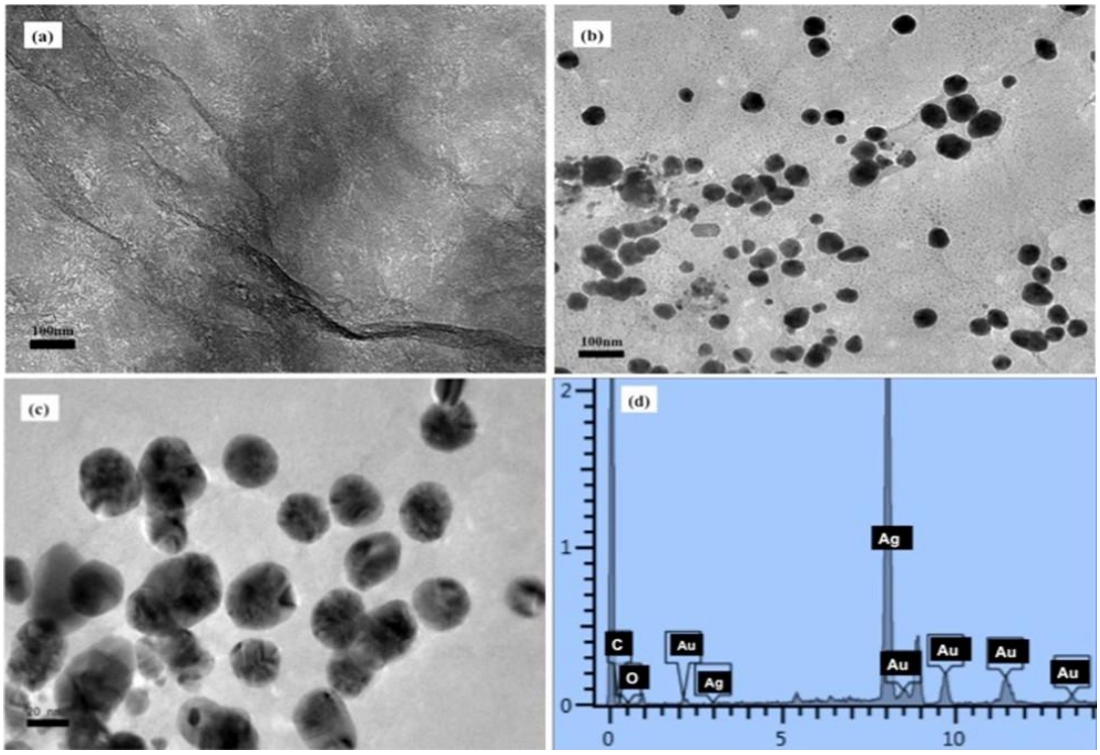

Figure 4. High resolution transmission electron microscopy of (a) rGO, (b) AgAu/rGO, (c) AgAu/rGO at 20nm and (d) EDX analysis of AgAu/rGO

Khalil and co researchers also stated that the unknown peaks emerged in the pattern that marked with X in the diffraction peak of AgAu/rGO, could be due to the crystalline bioorganic compound from the reduction process in which similar with the current result [41]. From the Joint Committee on Powder Diffraction Standards, JCPDS card number 07-0783 for Ag and 07-0784 for Au nanoparticles, the 2θ values of Ag and Au alloys are very contiguous to each other since both have a very similar lattice constant [43]. From these results, it's confirmed that Ag and Au nanoparticles were formed on the surface of reduced graphene oxide (rGO) during the chemical reduction process [44]. However, Ag and Au elemental ratio of the bimetallic nanoparticles is difficult to determine by XRD analysis as the lattice constant for Ag and Au nanoparticles are comparable to each other.

The morphology of rGO and AgAu/rGO nanohybrids was further confirmed by HRTEM analysis and shown in Figure 4. It shows that a transparent

sheetlike structure with wrinkles and crumbling silk veil wave on the surfaces and edges was observed in Fig. 4(a). These observation images of rGO were similar with the finding of Gebreegziabher and co-workers and suggesting the occurrence of few-layered graphene sheets is due to the flexibility and nature criteria of rGO [25,45]. Meanwhile, HRTEM image of bimetallic AgAu/rGO nanohybrids in Figure 4(b) and (c) shows that these nanoparticles were uniformly distributed on the surface of reduced graphene oxide and have a 25 nm - 40 nm of particles size with spherical shapes [46]. This finding agrees with previous studies that reported a 20 nm - 30 nm of Ag:Au bimetallic nanoparticles with same volume ratio were synthesized using chemical reduction method and Ag and Au particles were homogenously formed [47]. The elemental analysis was carried out using energy dispersive X-ray spectroscopy (EDX). EDX spectrum of each product in Figure 4(d) also revealed the existence of C, O, Ag and Au elements on the surface of rGO. Although some localized clustering is observed in the TEM image, analysis of multiple regions confirms that the Ag-Au nanoparticles are generally well distributed on the rGO surface, and the apparent non-uniformity is mainly due to sheet overlapping and imaging contrast effects.

Electrochemical Measurements

Figure 5 shows the typical cyclic voltammetry of the rGO/ITO electrode in 0.1 M PBS solutions at pH 7.0 in the absence and presence of 5 mM glucose in the potential window from -0.75 to 0.50 V at 50 $mV.s^{-1}$. Without addition of glucose, a redox peaks at -0.4 and +0.225V were observed to have ~0.51 $mA.cm^{-2}$ of current density. However, with addition of 5 mM glucose, a pair of defines redox peaks at -0.43 and +0.25 V appeared with the small redox peak currents density approximately ~0.53 $mA.cm^{-2}$ which relatively higher than absence of glucose. Here in, observation on the redox peak currents of rGO/ITO were enhanced compared to the bare ITO, approximately at ~0.5 $mA.cm^{-2}$ after addition of glucose. The result is in good agreement with the findings by previous studies, in which this increment could be attributed to the presence of rGO layer on electrode surface with good electrical conductivity and fast electrode transfer [48].

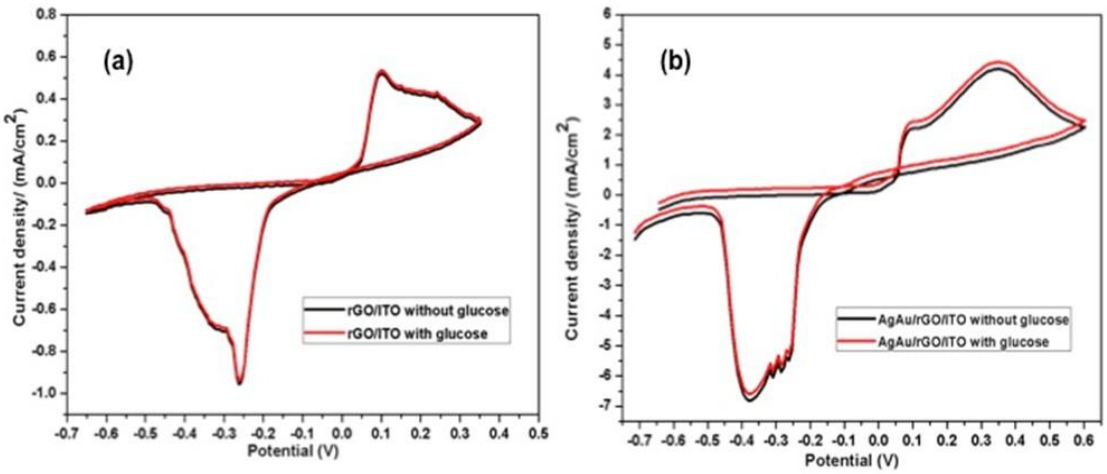

Figure 5. CV recorded on (a) rGO (b) AgAu/rGO nanohybrids, drop-casted on ITO electrode. Black curve is for without glucose and the red curve is for 4.0 mM glucose. The electrolyte was 0.1 M PBS solutions

Figure 5 shows voltammetric curve of AgAu/rGO/ITO (black curve) in 0.1 M PBS solutions in the absence of glucose. Two pairs oxidation peaks were observed at +0.1 V and +0.33 V on the anodic peak potential and a reduction peak at -0.38 V on the cathodic peak potential, respectively. After the addition of glucose (red curve), an oxidation peaks were observed shift to the more negative potential at +0.08 V and a broad oxidation peak at +0.3 V. However, the reduction peak maintains the same potential. In the presence of glucose, a small increment in peak current density approximately at ~4.5 $mA.cm^{-2}$ were observed at AgAu/rGO/ITO electrode. Interestingly, the height of the peak current density of AgAu/rGO electrode with

bimetallic nanoparticles significantly improved compared to the rGO electrode. As reported from the previous literature, oxidation of dopamine (DA) greatly improved due to the fast electron transfer kinetics between Ag-Au bimetallic nanoparticles at 1:1 ratio compared to the individual rGO, in which in good agreement with this result and observation [49]. From the observations obtained from cyclic voltammetry, it clearly shows that AgAu bimetallic nanoparticles decorated rGO on ITO electrode certainly had a remarkable enhancement in the electrochemical behaviour compared to rGO itself under the same experimental conditions. The reason for enhancing in peak current density in AgAu/rGO was attributed to the synergistic and catalytic effect of Ag and Au nanoparticles and by the large surface area of rGO itself [50].

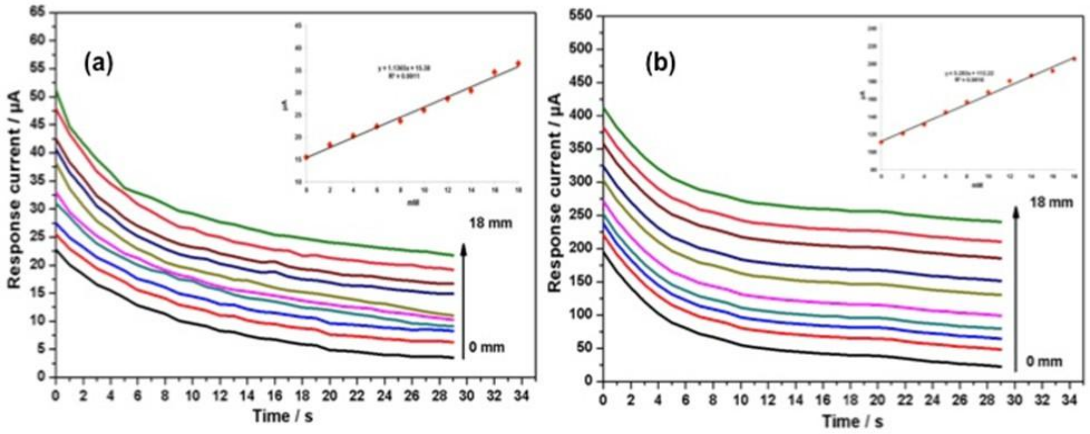

Figure 6. Amperometric response for 0 - 18 mM glucose concentrations on (a) rGO/ITO and (b) AgAu/rGO/ITO. Inset image shows calibration curves for respective samples showing current variation with concentration

Table 2. Comparison of sensor behavior of bimetallic nanocomposite based non-enzymatic glucose sensors

Electrode	Sensitivity ($\mu A.mM^{-1}.cm^{-2}$)	LOD (µM)	Linear range (mM)	Reference
HAg/PtNPs-rGO	129.32	1.8	0.003 - 7.72	[53]
Nanoporous Au/CuO	374	2.8	0 to 12	[54]
PtPb/Ti	10.18	-	0 to 16	[55]
PtAu/MWCNT	10.71	10	0 to 24	[56]
PtPd/MWCNT	112	31	0.062 - 14.07	[57]
Au–Ru/Chitosan/GCE	240	1.7	0 to 6	[58]
Pt-Au alloy/Si substrate	352	6	6 µM - 11 mM	[59]
AgAu/rGO/ITO	428	1.5	0 to 18	Current work

From the cyclic voltammetry studies, it was found that the well-defined oxidation peak of all electrodes toward glucose oxidation was in the range of +0.20 V to +0.45 V. The +0.25 V was selected as the optimized detection potential to evaluate the sensor behaviour of other electrodes as it gives higher response toward glucose. Figure 6(a) and (b) represent amperometric response for rGO/ITO and AgAu/rGO/ITO electrode toward glucose concentration in 0.1 M PBS solutions. The calibration curve observed in the inset in each figure showed the proposed electrode gives a linear dependence ($R^2 > 0.99$) in the glucose concentration range of 2 mM - 18 mM. As can be seen, all electrodes generate a plateau current signal linearly increasing along with glucose concentration increment, and reach steady state within 30 s. The sensitivity and limit of detection at a signal to noise ratio of 3 (S/N = 3) were noted to be 428 $\mu A.mM^{-1}.cm^{-2}$ and 1.5 µM for

AgAu/rGO/ITO respectively (Figure 6(a)). In contrary, in case for rGO/ITO (Figure 6(b)), the sensitivity and limit of detection was obtained at 55 $\mu A.mM^{-1}.cm^{-2}$ and 3.8 µM for rGO/ITO, respectively. rGO/ITO exhibited a small value of current response and detection limit after the addition of glucose. Interestingly, after Ag and Au NPs were decorated on rGO surface, AgAu/rGO give a high response to successive addition of glucose compared to rGO. This result thus confirms that a combination of bimetallic nanoparticles possesses excellent electrochemical behavior of glucose detection.

In alkaline medium, glucose is first adsorbed onto the Ag-Au active sites, where surface metal-hydroxide species facilitate its oxidation to gluconolactone with the release of electrons. In bimetallic systems, the electronic interaction between Ag and Au modifies the surface charge distribution, improving intermediate adsorption and accelerating oxidation kinetics compared to single-metal catalysts. The generated electrons are rapidly transferred through the conductive rGO network to the current collector, producing an enhanced electrochemical response. Such synergistic electronic modulation and improved charge transfer behavior in noble metal bimetallic catalysts have been widely reported in recent studies on non-enzymatic glucose sensing [51,52].

The comparison of our results with the recent reported bimetallic nanoparticles based on non-enzymatic glucose sensors is presented in Table 2. It is noteworthy that AgAu/rGO/ITO electrode exhibits relatively wider detecting linear range toward glucose up to 18 mM and high sensitivity than that of most bimetallic nanoparticles based non-enzymatic glucose sensors. As reported from the previous study by Wang and co-researchers, the high sensitivity of the response electrode toward glucose is attributed to the significant synergistic catalytic effect of the Ag and Au nanoparticles and large surface area of rGO, which offers a stable substrate for the bimetallic Ag-Au nanoparticles to promote and enhance the electron transfer between the electrode and detection molecules [53].

The synergistic effect between Ag and Au arises from electronic interaction within the bimetallic structure, which modifies the surface electronic density and enhances glucose adsorption and oxidation kinetics. Ag contributes strong catalytic activity toward glucose oxidation, while Au improves stability and resistance to surface poisoning. The combination of both metals therefore promotes faster electron transfer, lowers overpotential, and increases the number of active catalytic sites compared to their monometallic counterparts. These synergistic effects collectively enhance sensitivity, improve current response, and contribute to better stability and reliability of the final glucose sensor, making the Ag-Au/rGO system more suitable for practical sensor development.

4. CONCLUSIONS

In summary, we demonstrate a simple chemical route for synthesis of silver gold nanoparticles decorated on reduced graphene oxide. The nanohybrids have proved to be superior catalyst material for electrochemical sensor applications, especially in detecting glucose. The total response of the sensor has significantly enhanced as compared to rGO with 428 $\mu A.mM^{-1}.cm^{-2}$ and limit of detection 1.3 µM. The enhanced electrochemical performance was attributed to the synergistic combination effect of the Ag and Au nanoparticles with the large surface area of rGO. Furthermore, the sensor exhibited a wide linear range between 0 - 18 mM, in which the result proves potential use of AgAu/rGO in developing non-enzymatic glucose sensor detection. The novelty of this work lies in the integration of a simple citrate-reduction strategy with a direct comparative evaluation between rGO and Ag-Au/rGO electrodes, allowing the intrinsic contribution of the bimetallic nanoparticles to glucose sensing performance to be clearly demonstrated.

5. ACKNOWLEDGEMENTS

The authors would like to express gratitude to University Putra Malaysia (UPM) and Fundamental research grant schemes (FRGS) from the Ministry of Education (MOHE) for the financial supports given to conduct the research work under FRGS grant 03-01-15-1638FR.

6. NOMENCLATURE

h	heat transfer coefficient	$(W.m^{-2}.K^{-1})$
k	thermal conductivity	$(W.m^{-1}.K^{-1})$
Nu	Nusselt number, (Nu = hL/k)	

7. REFERENCES

[1] Novoselov, K. S., Geim, A. K., Morozov, S. V., Jiang, D., Zhang, Y., Dubonos, S. V., Grigorieva, I. V., and Firsov, A. A., 2004, Electric Field Effect in Atomically Thin Carbon Films, Science (80), 306 (5696), 666–669.

[2] Rather, J. A., Pilehvar, S., and De Wael, K., 2014, A graphene oxide amplification platform tagged with tyrosinase-zinc oxide quantum dot hybrids for the electrochemical sensing of hydroxylated polychlorobiphenyls, Sensors Actuators, B Chem., 190, 612–620.

[3] Zhou, W., Ding, C., Jia, X., Tian, Y., Guan, Q., and Wen, G., 2015, Self-assembly of Fe2O3/reduced graphene oxide hydrogel for high Li-storage, Mater. Res. Bull., 62, 19–23.

[4] Luo, J., Zhang, N., Lai, J., Liu, R., and Liu, X., 2015, Tannic acid functionalized graphene hydrogel for entrapping gold nanoparticles with high catalytic performance toward dye reduction, J. Hazard. Mater., 300, 615–623.

[5] Yan, J., Wei, T., Qiao, W., Shao, B., Zhao, Q., Zhang, L., and Fan, Z., 2010, Rapid microwave-assisted synthesis of graphene nanosheet/Co 3O4 composite for supercapacitors, Electrochim. Acta, 55 (23), 6973–6978.

[6] Stoller, M. D., Park, S., Yanwu, Z., An, J., and Ruoff, R. S., 2008, Graphene-Based ultracapacitors, Nano Lett., 8 (10), 3498–3502.

[7] Dikin, D. A., Stankovich, S., Zimney, E. J., Piner, R. D., Dommett, G. H. B., Evmenenko, G., Nguyen, S. T., and Ruoff, R. S., 2007, Preparation and characterization of graphene oxide paper, Nature, 448 (7152), 457–460.

[8] Kuila, T., Mishra, A. K., Khanra, P., Kim, N. H., & Lee, J. H., 2013, Recent advances in the efficient reduction of graphene oxide and its application as energy storage electrode materials. Nanoscale, 5(1), 52–71.

[9] Stankovich, S., Dikin, D. A., Piner, R. D., et al. 2007, Synthesis of graphene-based nanosheets via chemical reduction of exfoliated graphite oxide. Carbon, 45(7), 1558–1565.

[10] Yang, S., Liu, D., Meng, Q. B., Wu, S., & Song, X. M., 2018, Reduced graphene oxide-supported methylene blue nanocomposite as a glucose oxidase-mimetic for electrochemical glucose sensing. RSC Advances, 8(57), 32565–32573.

[11] Tamil Selvi Gopal, T., Alzahrani, K. E., Assaifan, A. K., et al. 2022, Reduced graphene oxide supported MXene based metal oxide ternary composite electrodes for non-enzymatic glucose sensor applications. Scientific Reports, 12, 20583.

[12] Jothi, L., Jayakumar, N., Jaganathan, S. K., and Nageswaran, G., 2018, Ultrasensitive and selective non-enzymatic electrochemical glucose sensor based on hybrid material of graphene nanosheets/graphene nanoribbons/nickel nanoparticle, Mater. Res. Bull., 98, 300–307.

[13] Toghill, K. E., and Compton, R. G., 2010, Electrochemical non-enzymatic glucose sensors: A perspective and an evaluation, Int. J. Electrochem. Sci., 5 (9), 1246–1301

[14] Wilson, R., & Turner, A. P. F. (1992). Glucose oxidase: an ideal enzyme. Biosensors and Bioelectronics, 7, 165–185.

[15] Wang, J. (2008). Electrochemical glucose biosensors. Chemical Reviews, 108, 814–825

[16] Chen, C. et al. (2013). Recent advances in electrochemical glucose biosensors. RSC Advances, 3, 4473–4491.

[17] Aparicio-Martínez, E. P., Vega-Rios, A., Osuna, V. & Dominguez, R. B., 2023, Salivary glucose detection with laser induced graphene/AgNPs non-enzymatic sensor. Biosensors 13(2), 207

[18] Marcano, D. C., Kosynkin, D. V, Berlin, J. M., Sinitskii, A., Sun, Z., Slesarev, A., Alemany, L. B., Lu, W., and Tour, J. M. Improved Synthesis of Graphene Oxide, 4 (8).

[19] Thanh, T. D., Balamurugan, J., Hwang, J. Y., Kim, N. H., and Lee, J. H., 2016, In situ synthesis of graphene-encapsulated gold nanoparticle hybrid electrodes for non-enzymatic glucose sensing, Carbon N. Y., 98, 90–98.

[20] Yang, D., Chen, B., Wang, K. & Chen, Y., 2025, Recent advances in non-enzymatic glucose sensors based on nanomaterials. Coatings 15(8), 892.

[21] Guo, S., Dong, S., and Wang, E., 2010, Three-dimensional Pt-on-Pd bimetallic nanodendrites

supported on graphene nanosheet: Facile synthesis and used as an advanced nanoelectrocatalyst for methanol oxidation, ACS Nano, 4 (1), 547–555.

[22] Shen, J., Li, T., Long, Y., Shi, M., Li, N., and Ye, M., 2012, One-step solid state preparation of reduced graphene oxide, Carbon N. Y., 50 (6), 2134–2140.

[23] Zainy, M., Huang, N. M., Vijay Kumar, S., Lim, H. N., Chia, C. H., and Harrison, I., 2012, Simple and scalable preparation of reduced graphene oxide-silver nanocomposites via rapid thermal treatment, Mater. Lett., 89, 180–183.

[24] Li, Y., Niu, X., Tang, J., Lan, M., and Zhao, H., 2014, A Comparative Study of Nonenzymatic Electrochemical Glucose Sensors Based on Pt-Pd Nanotube and Nanowire Arrays, Electrochim. Acta, 130, 1–8.

[25] Gebreegziabher, G. G., Asemahegne, A. S., Ayele, D. W., Dhakshnamoorthy, M., and Kumar, A., 2019, One-step synthesis and characterization of reduced graphene oxide using chemical exfoliation method, Mater. Today Chem., 12, 233–239.

[26] Vinoth, V., Wu, J. J., Asiri, A. M., and Anandan, S., 2017, Sonochemical synthesis of silver nanoparticles anchored reduced graphene oxide nanosheets for selective and sensitive detection of glutathione, Ultrason. Sonochem., 39 (March), 363–373.

[27] Parades, J. I., Villar-Rodil, S., Martínez-Alonso, A., and Tascón, J. M. D., 2008, Graphene oxide dispersions in organic solvents, Langmuir, 24 (19), 10560–10564.

[28] Vargas, C., Simarro, R., Reina, J. A., Bautista, L. F., Molina, M. C., and González-Benítez, N., 2019, New approach for biological synthesis of reduced graphene oxide, Biochem. Eng. J., 151 (July), 107331.

[29] Yuan, W., Gu, Y., and Li, L., 2012, Green synthesis of graphene/Ag nanocomposites, Appl. Surf. Sci., 261, 753–758.

[30] Xu, Z., Gao, H., and Guoxin, H., 2011, Solution-based synthesis and characterization of a silver nanoparticle-graphene hybrid film, Carbon N. Y., 49 (14), 4731–4738.

[31] Luo, Z., Lu, Y., Somers, L. A., and Johnson, A. T. C., 2009, High yield preparation of macroscopic graphene oxide membranes, J. Am. Chem. Soc., 131 (3), 898–899.

[32] Devi, M. M., Puspal, S. R. S., and Pratik, M., 2015, Graphene – Metal Nanoparticle Hybrids: Electronic Interaction Between Graphene and Nanoparticles, Trans. Indian Inst. Met., 0–5.

[33] Dinh, D. A., Hui, K. S., Hui, K. N., Cho, Y. R., Zhou, W., Hong, X., and Chun, H. H., 2014, Green synthesis of high conductivity silver nanoparticle-reduced graphene oxide composite films, Appl. Surf. Sci., 298, 62–67.

[34] Yao, H., Jin, L., Sue, H.-J., Sumi, Y., and Nishimura, R., 2013, Facile decoration of Au nanoparticles on reduced graphene oxide surfaces via a one-step chemical functionalization approach, J. Mater. Chem. A, 1, 10783–10789.

[35] Panácek, A., Kvítek, L., Prucek, R., Kolár, M., Vecerová, R., Pizúrová, N., Sharma, V. K., Nevecná, T., and Zboril, R., 2006, Silver colloid nanoparticles: Synthesis, characterization, and their antibacterial activity, J. Phys. Chem. B, 110 (33), 16248–16253.

[36] Li, X., Jiang, L., Zhan, Q., Qian, J., and He, S., 2009, Localized surface plasmon resonance (LSPR) of polyelectrolyte-functionalized gold-nanoparticles for bio-sensing, Colloids Surfaces A Physicochem. Eng. Asp., 332 (2–3), 172–179.

[37] Link, S., & El-Sayed, M. A. (1999). Size and temperature dependence of the plasmon absorption of colloidal gold nanoparticles. J. Phys. Chem. B, 103, 4212–4217.

[38] Jain, P. K., Lee, K. S., El-Sayed, I. H., & El-Sayed, M. A. (2006). Calculated absorption and scattering properties of gold nanoparticles. J. Phys. Chem. B, 110, 7238–7248

[39] Šimšíková, M., Bartoš, M., Keša, P., and Šikola, T., 2016, Green approach for preparation of reduced graphene oxide decorated with gold nanoparticles and its optical and catalytic properties, Mater. Chem. Phys., 177, 339–345.

[40] De, A. C. M., 2015, Graphene oxide-silver nanocomposite as a promising biocidal agent against methicillin-resistant Staphylococcus aureus.

[41] Khalil, M., and Sabry, D., 2018, Green synthesis of silver, gold and silver-gold nanoparticles: Characterization, antimicrobial activity and cytotoxicity abstract, (October).

[42] Holden, M. S., Nick, K. E., Hall, M., Milligan, J. R., Chen, Q., and Perry, C. C., 2014, Synthesis and catalytic activity of pluronic stabilized silver-gold bimetallic nanoparticles, RSC Adv., 4 (94), 52279–52288.

[43] Yallappa, S., Manjanna, J., and Dhananjaya, B. L., 2015, Phytosynthesis of stable Au, Ag and Au-Ag alloy nanoparticles using J. Sambac leaves extract, and their enhanced antimicrobial activity in presence of organic antimicrobials, Spectrochim. Acta - Part A Mol. Biomol. Spectrosc., 137 (1), 236–243.

[44] Bykkam, S., Ahmadipour, M., Narisngam, S., Kalagadda, V. R., and Chidurala, S. C., 2015, RETRACTED: Extensive Studies on X-Ray Diffraction of Green Synthesized Silver Nanoparticles, Adv. Nanoparticles, 4 (1), 1–10.

[45] He, H., and Gao, C., 2011, Graphene nanosheets decorated with Pd, Pt, Au, and Ag nanoparticles: Synthesis, characterization, and catalysis applications, Sci. China Chem., 54 (2), 397–404.

[46] Dhara, K., Ramachandran, T., Nair, B. G., and Babu, T. G. S., 2015, Single step synthesis of Au – CuO nanoparticles decorated reduced graphene oxide for high performance disposable nonenzymatic glucose sensor, J. Electroanal. Chem., 743, 1–9.

[47] Mailu, S. N., Waryo, T. T., Ndangili, P. M., Ngece, F. R., Baleg, A. A., Baker, P. G., and Iwuoha, E. I., 2010, Determination of anthracene on Ag-Au alloy nanoparticles/overoxidized-polypyrrole composite modified glassy carbon electrodes, Sensors (Switzerland), 10 (10), 9449–9465.

[48] Li, Z., Zhang, W., Guo, J., Yang, B., and Yuan, J., 2015, Improved synthesis of fluffy and wrinkled reduced graphene oxide for energy storage application, Vacuum, 117, 35–39.

[49] Arvinte, A., Crudu, I., Doroftei, F., Timpu, D., and Pinteala, M., 2018, Electrochemical codeposition of silver-gold nanoparticles on CNT-based electrode and their performance in electrocatalysis of dopamine, J. Electroanal. Chem., 829 (October), 184–193.

[50] Shi, Q., Diao, G., and Mu, S., 2014, The electrocatalytic oxidation of glucose on the bimetallic Au-Ag particles-modified reduced graphene oxide electrodes in alkaline solutions, Electrochim. Acta, 133, 335–346.

[51] Chen, J. et al. (2021). Glucose-oxidase-like catalytic mechanism of noble metal nanozymes. Nature Communications, 12, 3375.

[52] Zhang, W. et al. (2023). Research progress of electrode materials for non-enzymatic glucose electrochemical sensors. Sensors & Diagnostics, 2, 1–20.

[53] Wang, C., Sun, Y., Yu, X., Ma, D., Zheng, J., Dou, P., Cao, Z., and Xu, X., 2016, Ag–Pt hollow nanoparticles anchored reduced graphene oxide composites for non-enzymatic glucose biosensor, J. Mater. Sci. Mater. Electron., 27 (9), 9370–9378.

[54] Xiao, X., Wang, M., Li, H., Pan, Y., and Si, P., 2014, Non-enzymatic glucose sensors based on controllable nanoporous gold/copper oxide nanohybrids, Talanta, 125, 366–371.

[55] Wang, J., Thomas, D. F., and Chen, A., 2008, Nonenzymatic electrochemical glucose sensor based on nanoporous PtPb networks, Anal. Chem., 80 (4), 997–1004.

[56] Ryu, J., Kim, K., Kim, H. S., Hahn, H. T., and Lashmore, D., 2010, Intense pulsed light induced platinum-gold alloy formation on carbon nanotubes for non-enzymatic glucose detection, Biosens. Bioelectron., 26, 602–607.

[57] Chen, K., Pillai, K. C., Rick, J., Pan, C., Wang, S., Liu, C., and Hwang, B., 2012, Biosensors and Bioelectronics Bimetallic PtM (M = Pd, Ir) nanoparticle decorated multi-walled carbon nanotube enzyme-free, mediator-less amperometric sensor for H_2O_2, Biosens. Bioelectron., 33 (1), 120–127.

[58] Shim, J. H., Cha, A., Lee, Y., and Lee, C., 2011, Nonenzymatic amperometric glucose sensor based on nanoporous gold/ruthenium electrode, Electroanalysis, 23 (9), 2057–2062.

[59] Li, C., Wang, H., and Yamauchi, Y., 2013, Electrochemical deposition of mesoporous Pt-Au alloy films in aqueous surfactant solutions:

Towards a highly sensitive amperometric glucose sensor, Chem. - A Eur. J., 19 (7), 2242–2246.